Current Journal of Applied Science and Technology

39(32): 110-123, 2020; Article no.CJAST.61853
ISSN: 2457-1024
(Past name: British Journal of Applied Science & Technology, Past ISSN: 2231-0843, NLM ID: 101664541)

Suction Stress in Unsaturated Soils Considering Hydraulic Hysteresis

J. Ramírez Jiménez[1], J. M. Horta Rangel[1*], M. L. Pérez Rea[1], E. Rojas González[1], T. Lopez Lara[1] and J. B. Hernandez Zaragoza[1]

[1]Department of Graduate Engineering, Universidad Autónoma de Querétaro, Cerro de las Campanas, Querétaro, Qro. C.P. 76010, México.

Authors' contributions

Author JRJ has designed the study, wrote the protocol and wrote the first draft of the manuscript. Author JMHR has supervised whole research. Authors MLPR and ERG managed the analyses of the study. Authors JBHZ and TLL have managed the literature searches. All authors read and approved the final manuscript.

Article Information

DOI: 10.9734/CJAST/2020/v39i3231007
Editor(s):
(1) Dr. Nhamo Nhamo, Zimbabwe Open University, Zimbabwe.
Reviewers:
(1) P. Bindiya, Andhra University, India.
(2) Ying Feng, South China University of Technology, China.
Complete Peer review History: http://www.sdiarticle4.com/review-history/61853

Original Research Article

Received 02 September 2020
Accepted 07 October 2020
Published 26 October 2020

ABSTRACT

Aims: To develop a flow-moisture model that allows determining the variation of suction over time, as well as the suction stresses, using the finite element method in a two-dimensional model of unsaturated soil through an analogy with a transient thermal problem.
Study Design: The variables used in this study were soil suction, hydraulic conductivity, diffusivity and degree of saturation which was represented as the χ parameter of the Bishop's effective stress equation.
Place and Duration of Study: Graduate Engineering Department, Universidad Autónoma de Querétaro, between November 2019 and August 2020.
Methodology: To establish the model, experimental Soil-Water Retention Curve was taken from Galaviz (2016). With this information, the curves of hydraulic conductivity and diffusivity were calculated with the methods of Fredlund et al. (2012) and Li (1996). In ANSYS 19.2, an analogous transient thermal analysis was run to determine suction changes over time in a 12 x 2.4 meters two-dimensional medium with an impermeable membrane at the center of its surface which was 4.8

**Corresponding author: E-mail: jaimehorta@prodigy.net.mx, horta@uaq.mx;*

meters long. Through these suction changes, the hydraulic hysteresis algorithm presented by Zhou et al. (2012) was used to calculate the respective degrees of saturation, which were considered as the χ parameter to obtain the suction stresses.
Results: The changes in soil suction, degree of saturation and suction stress were properly modeled.
Conclusion: When considering the hydraulic hysteresis cycles, both spatial and temporal variations behaved in a similar way in the χ parameters as well as in the suction stresses. Such stresses depended on the analysis period, increasing in the dry season, according to the precipitation-evapotranspiration model, and decreasing in the wetting season. A time lag was observed between the maximum and minimum stresses as greater depths were studied. Along the horizontal axis, considering the same depth, the stresses varied more in the areas adjacent to the impermeable membrane, while at the center this variation was practically null.

Keywords: Soil suction; hysteresis; unsaturated soil; computer modeling; suction stress.

1. INTRODUCTION

Unsaturated soil mechanics is different from the classical soil mechanics or saturated soil mechanics, since the problems in the first one are non-linear in nature and take the form of partial differential equations that require an iterative method to be solved [1].

The non-linearity of the equations is due to the number of variables which depend on a single one. In unsaturated soil mechanics, soil suction affects the hydraulic and mechanical behavior because variables like degree of saturation, permeability, diffusion coefficient and elastic modulus depend on soil suction.

Coupled models of unsaturated soils associate the hydraulic and mechanical behavior, the hydraulic model determines the evolution of the degree of saturation and the mechanical one determines the evolution of stresses and deformations. Both are related since the degree of saturation has a significant effect on the internal bonding stresses that act on the contact areas between soil particles; deformations affect the behavior of water retention by changing the pore size distribution [2].

To predict the soil response it is essential to use the concept of effective stress (σ'), which is defined as the stress acting on the solid particles and is a function of the net stress ($\sigma - u_a$), matric $ua{-}uw$) and a parameter χ. Equation $\sigma' = (\sigma - u_a) + \chi\,(u_a - u_w)$ (1) shows the relationship between the previous variables. Notice that the effective stress is essential in soil mechanics, since the deformations are a function of the effective stress, not the total stress [3, 4].

$\sigma' = (\sigma - u_a) + \chi\,(u_a - u_w)$ (1)

$-ua+\chi\,ua-uw$ (1), the element $u_a - u_w$ refers to the matric suction or simply suction. This variable becomes necessary to predict unsaturated soil behavior and affects engineering soil properties directly or indirectly [5].

The product $\chi\,(u_a - u_w)$ is named suction stress, it affects the soil stress history and, consequently, the preconsolidation stress which is the boundary between elastic and plastic deformations [6].

Parameter χ is normally considered as a function of degree of the saturation (S_w), which is very favorable since there is a way to graphically relate these variables using the Soil-Water Retention Curve (SWRC). There are several candidates of the equation for parameter χ, Table 1 shows some of the most important, in this work the proposal by Öberg and Sälfors [7] of considering the parameter equal as the degree of saturation is considered.

It is not enough to evaluate the SWRC to determine the stresses generated by soil suction, also hydraulic hysteresis must be considered in the calculations. Intermediate drying and wetting cycles generate scanning curves inside the SWRC following infinite different paths, but their limit are the SWRC main branches, which means that scanning curves are asymptotic to SWRC [11].

The programming language used to write the model algorithm is ANSYS Parametric Design Language (APDL). This has the particularity of having table parameters (variables), which are similar to an array but they allow the obtention of

Table 1. Proposals of effective stress parameter in Bishop's equation

Equation	Author
$\chi = S_w$	Öberg and Sälfors [7].
$\chi = (S_w)^k$ where k is fitting parameter	Vanapalli, Fredlund, Pufahl and Clifton [8].
$\chi = \left(\frac{s}{s_{ae}}\right)^{0.55}$ where s_{ae} is the air entry value	Khalili and Khabbaz [9].
$\chi = f^s + S_w^u f^u$ where f_s is the saturated fraction, f_u is the unsaturated fraction and S_w^u is the degree of saturation of the unsaturated fraction.	Rojas [10].

elements that are not explicitly in the table through linear interpolation [12].

2. MATERIAL AND METHODS / EXPERIMENTAL DETAILS / METHODOLOGY

The moisture-flow model for unsaturated soils is written in APDL in order to use the ANSYS 19.2 program as a compiler and to make use of the finite elements library available within the program for the analogous transient thermal analysis.

The hydraulic hysteresis algorithm is run with data from Viaene et al. (1994) [13] to calculate its correlation with equation (2) where r is the correlation coefficient, x is the experimental degree of saturation, y is the modeled degree of saturation evaluated at the suctions of experimental data, $\bar{x}$ and $\bar{y}$ are the means.

$$r^2 = \left(\frac{\sum(x-\bar{x})(y-\bar{y})}{\sqrt{\sum(x-\bar{x})^2 \sum(y-\bar{y})^2}}\right)^2 \quad (2)$$

The validation of the hysteresis model is significant because it can be used to calculate the parameter χ, which can be considered as the degree of saturation or a function of it.

The hydraulic hysteresis cycles that are used to determine the suction stresses were developed from the method presented by Zhou et al. (2012). This process considered the creation of an equation (3) which describes the path of the main curves, having the degree of saturation as a dependent variable, the suction as an independent variable as well as three fitting parameters: m, n and a, which are different for each path.

$$S_e = \left[1 + \left(\frac{s}{a}\right)^m\right]^n \quad (3)$$

Equation (3) is relevant because it has an element that can be derived to calculate the slope at any point on the curve. This slope is used in the calculation of the scanning curves inside the main branches of the SWRC.

However, the use of an equation that describes the relation between suction and degree of saturation becomes unnecessary when working with APDL since the table array parameters allow the obtention of intermediate values through interpolation. These intermediate values are helpful to calculate the slopes at any point of the main branches; when dividing a small increment of degree of saturation by a small increment of suction, the program obtains the slopes.

In Fig. 1 the elements required to calculate the degree of saturation due to a change in suction in any direction (drying or wetting) are identified.

The process is iterative, starting from an initial suction and moving towards the final suction. This method is represented by equation (4), which is used when the final suction is smaller than the initial one (when the soil moisture is increasing), and equation (5) for the opposite case.

$$\frac{(\partial S_{es})}{\partial s}(wetting) = \left(\frac{S_w}{s}\right)^b \left(\frac{\partial S_{ew}}{\partial s}\right) \quad (4)$$

$$\frac{(\partial S_{es})}{\partial s}(drying) = \left(\frac{s_d}{s}\right)^{-b}\left(\frac{\partial S_{ed}}{\partial s}\right) \quad (5)$$

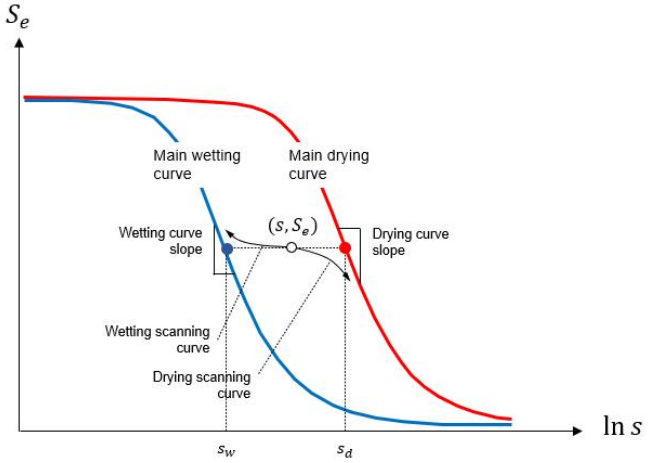

Fig. 1. Hydraulic hysteresis variables, modified from Zhou et al. 2012

The values of suction on the main curves (s_w and s_d) as well as the slopes at those points, change with each degree of saturation increment. Notice that b parameter is empirical, always positive, and the same value is adopted for both the drying and wetting path [14].

The behavior of the scanning curves is given in Fig. 2. The α node departs from the main drying curve and the β node departs from the main wetting curve; the values of suction and degree of saturation at the end of a cycle are the initial values of the next one.

The hydraulic hysteresis model from Zhou et al. (2012) needs suction values as input. Those values will be calculated using the finite element method. The 2-D domain (Fig. 3) is established with a length of 12 m and 2.4 m depth with the effect of precipitation-evapotranspiration on its surface, it also has an impermeable membrane going from x=3.6 m to x=8.4 m. The mesh is made up of squared elements of 0.1 m per side.

With 2,880 finite elements in the soil's domain, the model has 3,025 nodes, each one associated with a value of suction. Those values will change with the pass of time for 48 months of analysis.

The experimental data [15]–[17] are taken to simulate these processes. The soil was classified as an unsaturated high-plasticity clay obtained from Jurica in Querétaro city. Its properties are presented in Table 2.

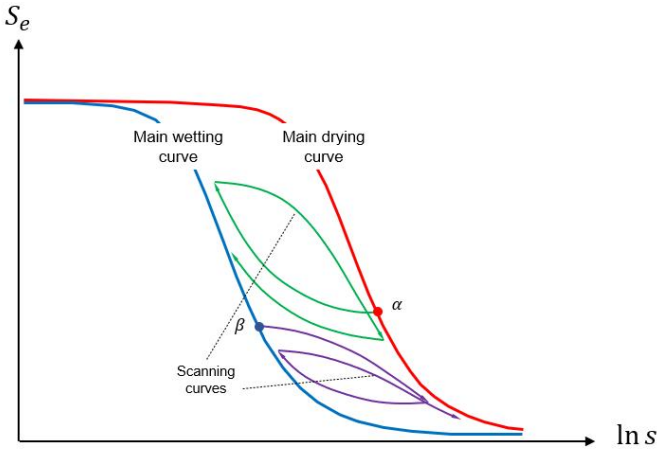

Fig. 2. Representation of the paths followed by hypothetical nodes with three hysteresis cycles

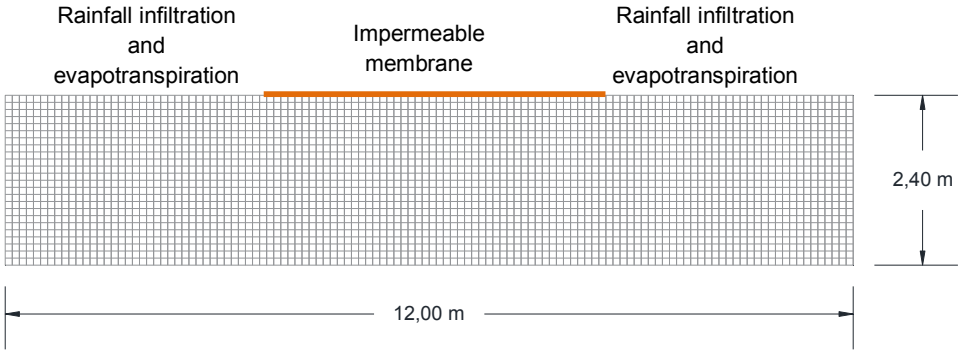

Fig. 3. Finite elements mesh of the soil's domain

Table 2. Soil's geotechnical properties used in the analysis [15]–[18]

Property	Symbol	Magnitude	Property	Symbol	Magnitude
Specific weight	γ_m	16.60 kN/m^3	Gravimetric water content	w	33%
Dry unit weight	γ_d	13.59 kN/m^3	Saturated permeability	k_s	1.37 x 10^{-7} m/s
Specific gravity	S_s	2.35	Liquid limit	LL	74.36%
Void ratio	e	1.31	Plastic limit	PL	28.57%
Porosity	n	0.57	Plasticity index	PI	45.79%
Degree of saturation	S_w	60.01%	Classification	USCS	CH
Volumetric water content	θ	34.04%	Clay activity	A	0.95

The analysis is made using an analogy of the suction behavior with a transient thermal analysis. The element used from the ANSYS finite elements library is the *PLANE55* element (which have four nodes with a single degree of freedom [19]).

Through the application of Darcy's law, the equations of continuity of moisture flow and assuming the soil body as homogenous and isotropic, the diffusion equation (6) can be obtained to describe the unsaturated moisture flow [20].

$$\frac{1}{\mathrm{D}}\frac{\partial s}{\partial t} = \frac{\partial^2 s}{\partial^2 x} + \frac{\partial^2 s}{\partial^2 y} + \frac{\partial^2 s}{\partial^2 z} + \frac{f(x,y,z,t)}{k_w} \quad (6)$$

Where:

$D = k_w/(c\rho_d)$ = diffusion coefficient
s = soil suction
t = time
k_w = hydraulic conductivity, a function of soil suction
$c = \Delta w/\Delta s$ = the moisture characteristic
ρ_d = dry density
x, y, z = the space coordinates
$f(x, y, z, t)$ = a source of moisture generated in the soil

The diffusion equation (6) has the same structure as the heat equation, so the variables to perform the analogous analysis are:

- Soil suction as the temperature.
- The hydraulic conductivity k_w as the thermal conductivity.
- The diffusion coefficient D as the reciprocal of specific heat capacity.

The diffusion coefficient is a function of hydraulic conductivity, which is a function of suction. To obtain the unsaturated hydraulic conductivity, equation (7) is applied [11].

$$k_w(\theta_w)_i = \frac{k_s}{k_{sc}} A_d \sum_{j=i}^{m} \left[(2j+1-2i)(u_a - u_w)_j^{-2}\right] \quad (7)$$

Where:

$k_w(\theta_w)_i$ = hydraulic conductivity for a specified volumetric water content θ_i corresponding to the i-th interval.

i = interval number that increases with decreasing water content.

k_s/k_{sc} = matching factor based on the measured saturated hydraulic conductivity and calculated hydraulic conductivity.

A_d = adjusting factor as a function of surface tension, density and absolute viscosity of water.
j = counter from i to m.
m = total number of intervals between the saturated volumetric water content and the lowest water content on the experimental SWRC.

The model adopted for seasonal precipitation-evapotranspiration (8) is cyclic cosinusoidal because it reported better results according to in situ suction data.

$$P(m) = 70\cos\left(\frac{\pi}{6}m - \varphi\right) \quad (8)$$

Where:

P = precipitation in millimeters
70 = is the amplitude of the function corresponding to a maximum precipitation of 70 mm
m = month of analysis, from 1 to 12
φ = phase angle = $\pi/2$

An equilibrium suction value is needed to assign initial values to every node. This is the limit value which does not change with depth, it was considered equal as 2,600 kPa, which is the suction at 4.5-meter depth according to Juricas's soil experimental data [15]. The suction changes with depth are presented in Fig. 4.

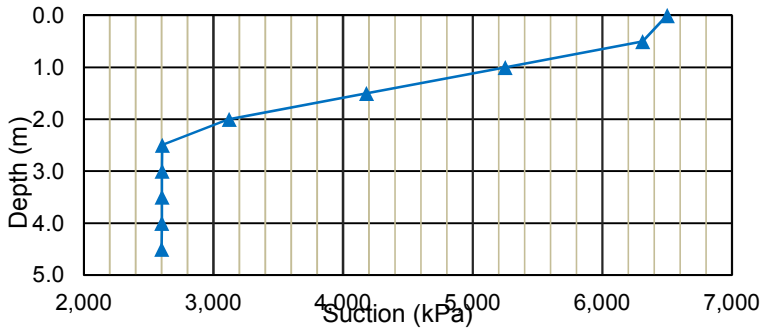

Fig. 4. Suction at different depths of Jurica's soil

Once established the specifications to determine the suction values, they will be store in a matrix named SUCTIE. That matrix will be used to obtain the degree of saturation due to changes in soil suction according to the previously described hydraulic hysteresis algorithm.

Each row represents a node of the finite element mesh and the columns are associated with time increasing from left to right. The structure of that matrix is represented in equation (9).

$$\text{SUCTIE} = \begin{matrix} \\ \text{Nodes} \\ \downarrow \end{matrix} \overset{\text{Time}\ \rightarrow}{\begin{pmatrix} s_{11} & s_{12} & \cdots & s_{1n} \\ s_{21} & s_{22} & \cdots & s_{2n} \\ \cdots & \cdots & \cdots & \cdots \\ s_{n1} & s_{n2} & \cdots & s_{nn} \end{pmatrix}} \quad (9)$$

Taking the suction matrix as input, the hydraulic hysteresis algorithm is used to determine the respective degrees of saturation and thus calculate a matrix (CHI) with these values, this new matrix has the same size as SUCTIE. The way the program work is represented in Fig. 5 and the structure of the output matrix with the degrees of saturation (CHI) is presented in equation (10).

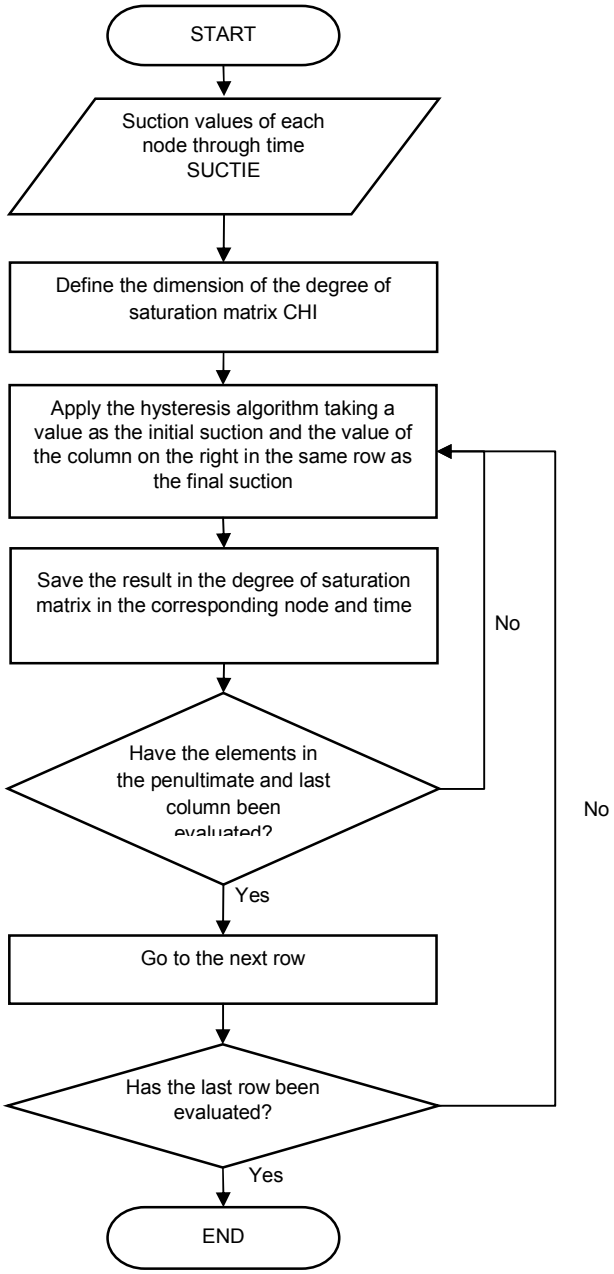

Fig. 5. Flowchart of the hydraulic hysteresis calculation to generate the degree of saturation matrix CHI

$$\text{CHI} = \begin{matrix} \\ \text{Nodes} \downarrow \end{matrix} \overset{\text{Time} \rightarrow}{\begin{pmatrix} S_{e11} & S_{e12} & \cdots & S_{e1n} \\ S_{e21} & S_{e22} & \cdots & S_{e2n} \\ \cdots & \cdots & \cdots & \cdots \\ S_{en1} & S_{en2} & \cdots & S_{enn} \end{pmatrix}} \tag{10}$$

Finally, a matrix with the same size as SUCTIE and CHI is dimensioned; the elements of SUCTIE are multiplied by their corresponding elements in CHI (considering them as the parameters χ) to obtain the matrix with the suction stresses, named SUC_STRESS, which is represented in equation (11).

$$\text{SUC\_STRESS} = \begin{matrix} \\ \text{Nodes} \downarrow \end{matrix} \overset{\text{Time} \rightarrow}{\begin{pmatrix} \chi S_{11} & \chi S_{12} & \cdots & \chi S_{1n} \\ \chi S_{21} & \chi S_{22} & \cdots & \chi S_{2n} \\ \cdots & \cdots & \cdots & \cdots \\ \chi S_{n1} & \chi S_{n2} & \cdots & \chi S_{nn} \end{pmatrix}} \tag{11}$$

The domain nodes were assigned with the same initial suction value, therefore the last period of drought-humidity-drought was used to apply the hydraulic hysteresis algorithm and also to obtain the suction stresses; such period comprised from month 34 to 46.

3. RESULTS AND DISCUSSION

Plots of the variables used for the analogous analysis are presented in Fig. 6; Fig. 6a is the experimental SWRC [16] and Figs. 6b and 6c represent the hydraulic conductivity and diffusion coefficient respectively, according to the equations presented in this text. In every plot the blue line corresponds to the main wetting curve and the red line corresponds to the main drying curve.

The transient thermal analysis takes suction, hydraulic conductivity and diffusivity (the last two related to suction) and it results in the SUCTIE matrix. Plots of the domain with intervals of suction at different times are given in Fig. 7. where variations in both the x and y axis are shown.

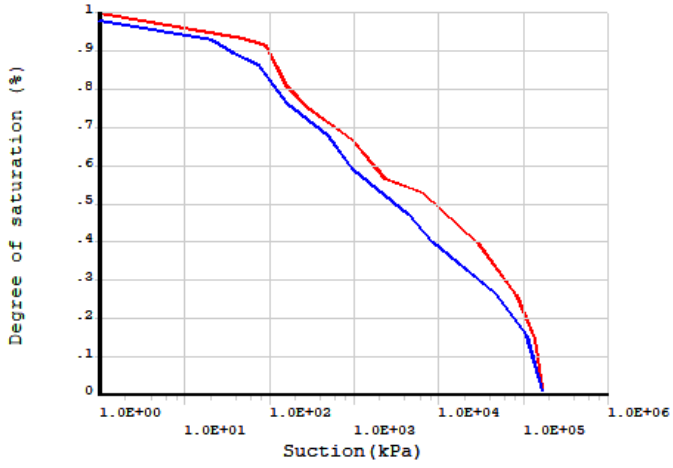

a)

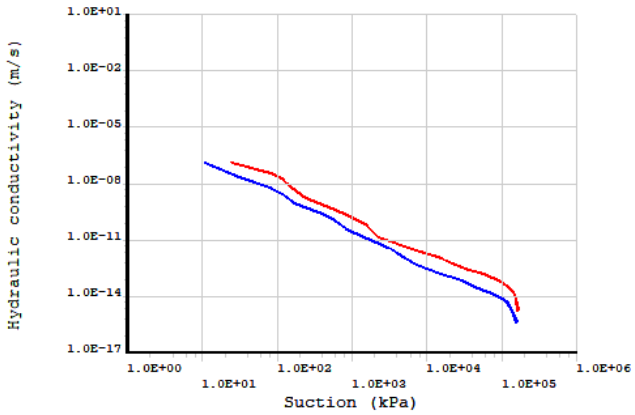

b)

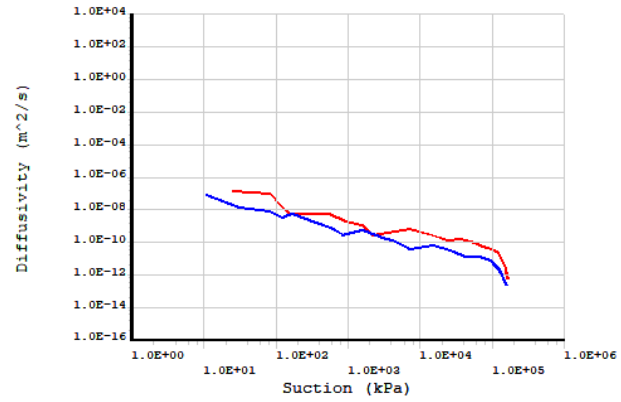

c)

Fig. 6. Variables employed to perform the analogous transient thermal analysis, a) SWRC, b) Hydraulic conductivity curve, c) Diffusivity curve

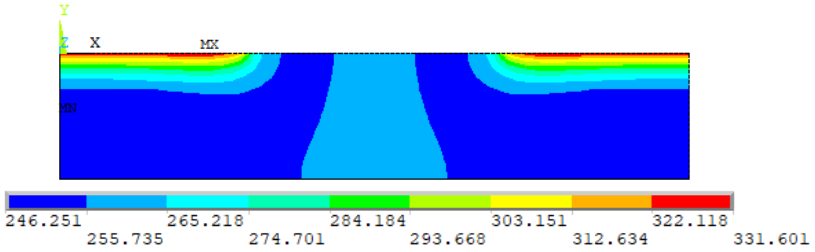

a)

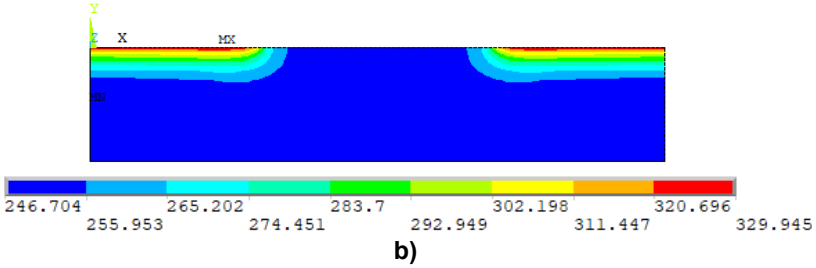

b)

Fig. 7. Suction values on soil's domain (x10 kPa), a) Month 34, b) Month 46. Generated in ANSYS 19.2

A contrast between the behavior of the hydraulic hysteresis model and experimental data from Viaene et al. (1994) is observed in Fig. 8. The squared of the correlation coefficient was calculated as 0.9993 and 0.9967 for the wetting and drying scanning curve respectively.

Considering the soil composed by finite elements, the algorithm developed is used to obtain the change in suction and degree of saturation at each finite element node over time. This information is stored in two matrices, each of 3025 rows per 48 columns; the rows correspond to the nodes of the elements and the columns represent different time periods, increasing month by month until reaching four years.

Regarding the information contained in the generated parameters, a portion of the matrices with the suction changes (SUCTIE) and degree of saturation changes (CHI) are presented in Tables 3 and 4 respectively. The matrices shown are consistent with the theory which dictates that when suction decreases, the degree of saturation increases and vice versa.

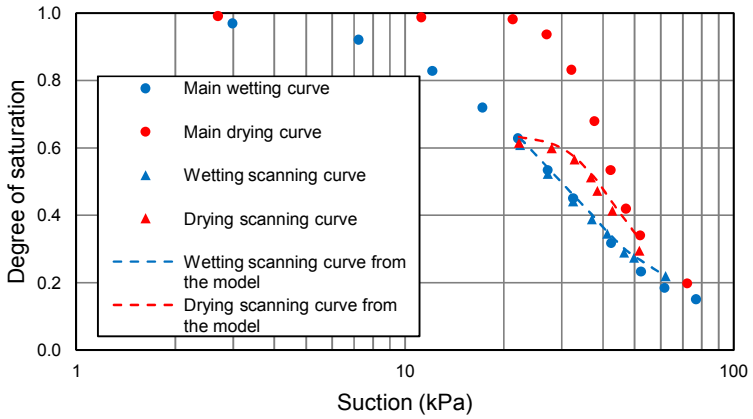

Fig. 8. Modeled scanning curves and scattered plot of main and scanning curves with data from Viaene et al. (1994)

Table 3. Portion of the SUCTIE matrix with suction values (kPa)

		Month of analysis					
		34	**35**	**36**	**…**	**45**	**46**
Node number	**1**	3,278.62	3,242.43	3,031.25	…	3,060.06	3,265.58
	2	2,497.76	2,493.43	2,491.26	…	2,514.48	2,508.99
	3	3,102.76	3,130.97	3,010.66	…	2,874.04	3,082.13
	…	…	…	…	…	…	…
	3024	2,497.50	2,493.26	2,491.29	…	2,514.21	2,508.69
	3025	2,497.39	2,493.16	2,491.18	…	2,514.12	2,508.61

Table 4. Portion of the CHI matrix with degree of saturation values

		Month of analysis					
		34	**35**	**36**	**…**	**45**	**46**
Node number	**1**	0.5574	0.5578	0.5603	…	0.5493	0.5468
	2	0.5633	0.5635	0.5636	…	0.5614	0.5617
	3	0.5488	0.5485	0.5498	…	0.5517	0.5491
	…	…	…	…	…	…	…
	3024	0.5633	0.5636	0.5637	…	0.5615	0.5617
	3025	0.5633	0.5636	0.5637	…	0.5615	0.5617

The elements of the matrix containing the suction stresses are obtained by multiplying the element (i, j) of the SUCTIE matrix by the element (i, j) of the CHI matrix, with i going from 1 to the total number of nodes and j from 1 to the total number of months. The matrix was named SUC_STRESS and is presented in Table 5.

The evolution of the suction stress over time for a given value on the horizontal axis at increasing depths is plotted in Fig. 9. Fig. 9a corresponds to the stresses in a location outside the impermeable membrane (x=1.8 m) and it shows the greatest variations with respect to depth; for Fig. 9b and 9c the analyzed nodes are located in x=3.6 m (at one edge of the impermeable membrane) and x=6.0 m (at the middle of the domain) respectively, showing both less variations than Fig. 9a. For Fig. 9c, the curve with the smaller suction stress values corresponds to the point on the surface, the greater the depth the greater the suction stress. In every plot of Fig. 9, the curve with the greatest amplitude corresponds to the node at the surface of the domain; the remaining curves with decreasing amplitude correspond to nodes of increasing depth with separation of 0.1 m.

Table 5. Portion of the SUC_STRESS matrix with suction stress values (kPa)

		Month of analysis					
		34	**35**	**36**	**…**	**45**	**46**
Node number	**1**	182.75	180.86	169.83	…	168.10	178.57
	2	140.70	140.51	140.42	…	141.17	140.92
	3	170.30	171.73	165.52	…	158.57	169.23
	…	…	…	…	…	…	…
	3024	140.69	140.51	140.43	…	141.16	140.91
	3025	140.69	140.51	140.42	…	141.16	140.91

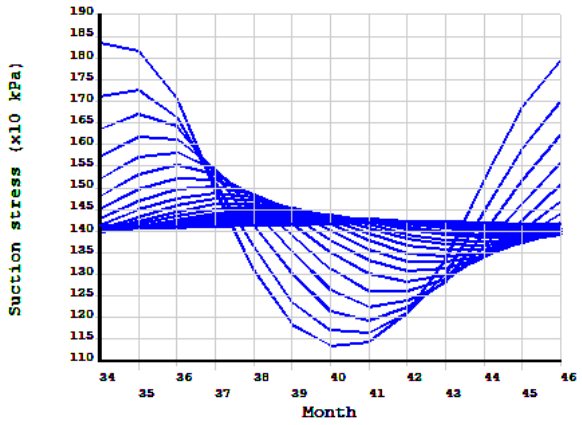

a)

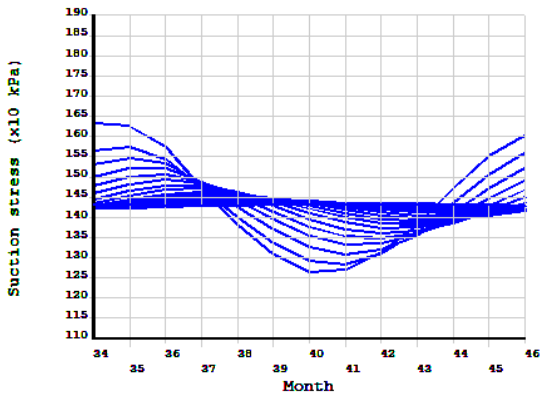

b)

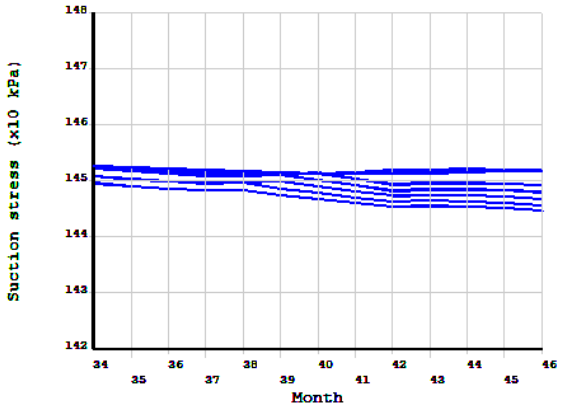

c)

Fig. 9. Evolution of suction stresses in a soil column, a) At x=1.8 m, b) At x=3.6 m, c) At x=6.0 m

It must be noticed that the maximum suction stress in a given node and time does not correspond to the maximum stress of other node at different depth at the same time. The maximum suction stresses of deeper nodes are delayed because of the diffusive process.

Fig. 10 shows the variations of suction stresses along the horizontal axis for different depths and time. As previously seen in Fig. 9, suction stresses are less changeable as depth increases, also horizontal location is significant since beneath the impermeable membrane the stresses remain nearly constant.

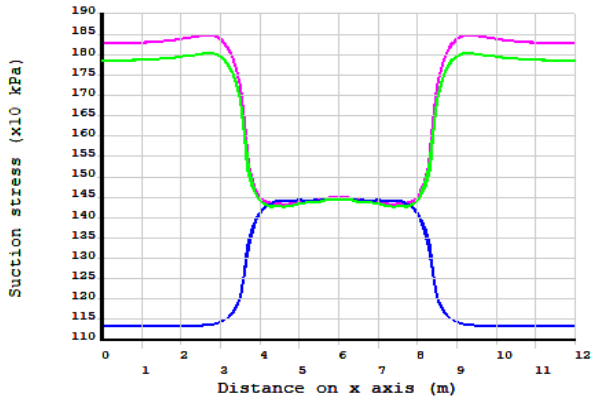

a)

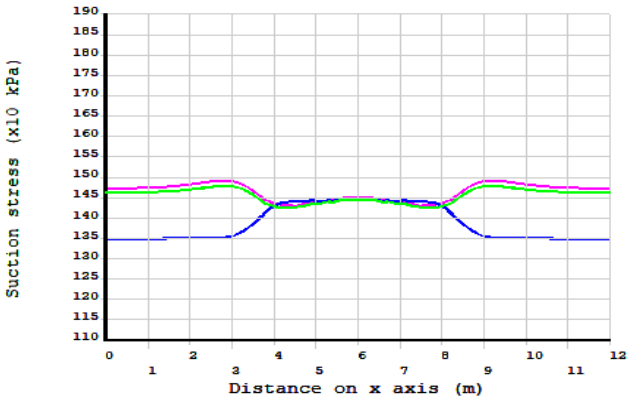

b)

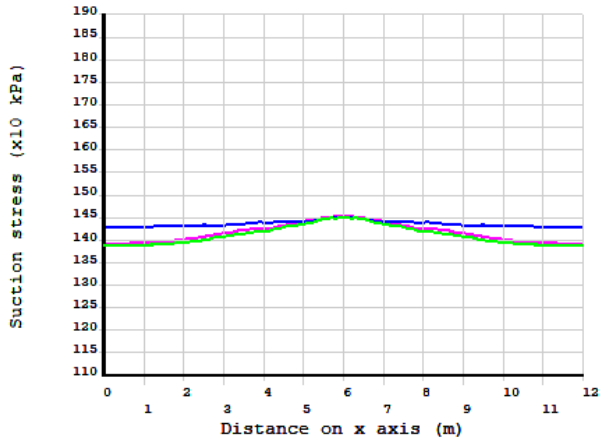

c)

Fig. 10. Suction stresses at 34 (green), 40 (blue) and 46 (purple) months, a) At 0.00 m depth, b) At 0.50 m depth, c) At 1.00 m depth

4. CONCLUSION

The results presented are a significant contribution in the numerical modeling of problems associated with the flow-moisture behavior of soils in unsaturated condition, since it takes into consideration the hydraulic hysteresis cycles for the determination of the suction stresses in the nodes of the domain.

The high correlation of experimental data and the calculated hydraulic hysteresis curves ensures its use as a predictive model with the possibility of being used not only to calculate the degree of saturation but also the parameter χ, since it can be considered as the degree of saturation or a function of it.

When considering the hydraulic hysteresis cycles, both spatial and temporal variations behaved in a similar way in the χ parameters as well as in the suction stresses. Such stresses depended on the analysis period, increasing in the dry season, according to the precipitation-evapotranspiration model, and decreasing in the wetting season. A time lag was observed between the maximum and minimum stresses as greater depths were studied.

Regarding the spatial location of the analysis point, we must consider both depth and horizontal location: the depth affects the stresses variations over time, a greater depth exhibits less variation; along the horizontal axis, considering the same depth, the stresses vary more in the areas adjacent to the impermeable membrane, while at the center this variation is practically null.

It should be noted that the stresses generated at greater depths could change dramatically if a source of moisture, such as a broken pipe, appears within the domain. This is beyond the scope of this paper but it could be the direction for future researches.

COMPETING INTERESTS

Authors have declared that no competing interests exist.

REFERENCES

1. Fredlund DG. Teaching unsaturated soil mechanics as part of the undergraduate civil engineering curriculum. Pan Am. Conf. Geotech. Eng. Educ. 2002;26–27.
2. Hu R, Chen YF, Liu HH, Zhou CB. A coupled stress-strain and hydraulic hysteresis model for unsaturated soils: Thermodynamic analysis and model evaluation. Comput. Geotech. 2015;63:159–170.
3. Bishop A. The principle of effective stress. Tek. Ukebl.1959;39:859–863.
4. Budhu M. Soil mechanics and foundations, 3rd ed. United States of America: Sons, John Wiley &, Inc; 2011.
5. Rahardjo H, Leong EC. Suction measurements. Geotech. Spec. Publ. 2006;147:81–104.
6. Brumund WF, Jonas E, Ladd CC. Estimating in situ maximum past (Preconsolidation) pressure of saturated clays from results of laboratory

Consolidometer Tests. in Special Report - National Research Council, Transportation Research Board. 1976;163:4–12.
7. Öberg AL, Sälfors G. A rational approach to the determination of the shear strength parameters of unsaturated soils. First Int. Conf. Unsaturated Soils. 1995;151–156..
8. Vanapalli SK, Fredlund DG, Pufahl DE, A. Clifton W. Model for the prediction of shear strength with respect to soil suction. Can. Geotech. J. 1996;33(3):379–392.
9. Khalili N, Khabbaz MH. A unique relationship for χ for the determination of the shear strength of unsaturated soils. Geotechnique. 1998;48(5):681–687.
10. Rojas E. Towards a unified soil mechanics theory. México: Bentham e Books; 2013.
11. Fredlund DG, Rahardjo H, Fredlund MD. Unsaturated soil mechanics in engineering practice. Hoboken, New Jersey: John Wiley & Sons, Inc; 2012.
12. ANSYS, ANSYS Parametric design language guide; 2019. [Online]. Available:https://ansyshelp.ansys.com/account/secured?returnurl=/Views/Secured/corp/v194/ans_apdl/Hlp_P_APDL3_11.html%23apdltbltyptlm8599. [Accessed: 24-Mar-2020].
13. Viaene P, Vereecken H, Diels J, Feyen J. A statistical analysis of six hysteresis models for the moisture retention characteristic. Soil Sci. 1994;157(6):345–355.
14. Zhou AN, Sheng D, Sloan SW, Gens A. Interpretation of unsaturated soil behaviour in the stress - Saturation space, I: Volume change and water retention behaviour. Comput. Geotech. 2012;43:178–187.
15. López Lara T. Resistencia al esfuerzo cortante en arcillas expansivas de Jurica, Querétaro. Universidad Autónoma de Querétaro; 1995.
16. Galaviz González R. Modelo acoplado (termo-mecánico) para suelos no saturados bajo el concepto de esfuerzos efectivos. Universidad Autónoma de Querétaro; 2016.
17. Galaviz González R, Horta Rangel J, Avalos Cueva D, Limón Covarrubias P, Robles Sotelos J. Hysteresis cycles prediction and their behavior on expansive soil-water retention curve. XVI Pan-American Conf. Soil Mech. Geotech. Eng., no. 2019;536–537.
18. Gallegos Fonseca G. Modelo probabilista para obtener la curva característica del suelo. Universidad Autónoma de Querétaro; 2011.
19. ANSYS. PLANE55. 2019. [Online]. Available:https://ansyshelp.ansys.com/account/secured?returnurl=/Views/Secured/corp/v194/ans_elem/Hlp_E_PLANE55.html. [Accessed: 26-May-2020].
20. Li J. Two dimensional simulation of a stiffened slab on expansive soil subject to a leaking underground water pipe. Geotech. Spec. Publ. 2006;147:2098–2109.

Peer-review history:
The peer review history for this paper can be accessed here:
http://www.sdiarticle4.com/review-history/61853